Accurate binding of sodium and calcium to phospholipid bilayers by effective inclusion of electronic polarization

Josef Melcr and Hector Martinez-Seara Monne

Institute of Organic Chemistry and Biochemistry, Academy of Sciences of the Czech Republic, Prague 6, Czech Republic

Jiří Kolafa

Department of Physical Chemistry, Institute of Chemical Technology, Prague 6, Czech Republic

Pavel Jungwirth

Institute of Organic Chemistry and Biochemistry, Academy of Sciences of the Czech Republic, Prague 6, Czech Republic and Department of Physics, Tampere University of Technology, P.O. Box 692, FI-33101 Tampere, Finland

O. H. Samuli Ollila*

Institute of Organic Chemistry and Biochemistry, Academy of Sciences of the Czech Republic, Prague 6, Czech Republic and Institute of Biotechnology, University of Helsinki

(Dated: November 16, 2017)

Binding affinities and stoichiometries of Na^+ and Ca^{2+} ions to phospholipid bilayers are of paramount significance in the properties and functionality of cellular membranes. For example, possible accumulation of ions at the membrane interface determines the interaction affinity with charged species. Current estimates of binding affinities and stoichiometries of cations are, however, controversial due to limitations in the available experimental and theoretical methods. Experimentally one can assess these parameters by titrating several membrane properties as a function of the ion concentration. However, the interpretation of the experiments relies on theoretical models, which give the best idealization of the ion binding as the direct experiments are not available. Classical molecular dynamics (MD) simulations provide details of the ion binding process with atomistic resolution, therefore offering all the necessary information to interpret experimental data without the need to resort to simplified models. However, the accuracy of the available lipid models when interacting with ions is not sufficient for such interpretation. In this work, we improve the binding details of Na^+ and Ca^{2+} ions to the 1-Palmitoyl-2-oleoyl-phosphatidylcholine (POPC) bilayer by implicitly including electronic polarization as a mean field correction, known as the electronic continuum correction (ECC). This is applied to the partial charges of a selected state of the art POPC lipid model for MD simulations. Our improved ECC-POPC model reproduces not only the experimentally measured structural parameters for the ion-free membrane, but also the response of lipid headgroup to a bound positive charge, and the binding affinities of Na^+ and Ca^{2+} ions. With our new model we also observe negligible binding of Na^+ ions to POPC bilayer and stronger interactions of Ca^{2+} primarily with phosphate oxygens, in agreement with the previous interpretations of the experimental spectroscopic data. On the other hand, the new model results in Ca^{2+} ions forming complexes with one to three POPC molecules with almost equal probabilities, suggesting more complex binding stoichiometry than simple models previously used to interpret the NMR data. The results of this work pave the way to quantitative MD simulations of complex biochemical systems with realistic electrostatic interactions in the vicinity of cellular membranes.

I. INTRODUCTION

Ion interactions with cellular membranes play a key role in critical biological processes [1, 2]. Ions, especially multivalent cations, modify general properties of the membrane which ultimately modulate their embedded transmembrane proteins [2–4]. Ions also have a more direct effect by modulating lipid–, protein–, and sugar–lipid interactions at the membrane surface. For example, Ca^{2+} is crucial in neural signal propagation. It promotes membrane fusion by bridging lipids in the vesicles carrying neurotransmitters and the neuron synapsis membrane [?]. Ca^{2+} also participates in the T-cell receptor activation. It induces the detachment of the positively charged cytosolic tails of the CD3 protein complex from the negatively charged intracellular membrane making it accessible for Lck protein [?]. A final example involving sugar-lipid interactions mediated by ions is that Ca^{2+} can modulate the presentation of the sugars found in the $PI(4,5)P_2$ lipid which ultimately modulates phospholipase C delta 1 pleckstrin homology domain (PLC δ1-H) [?]. Interestingly, this modulation is lost when using Mg^{2+} instead of Ca^{2+} illustrating the selectivity of these processes towards particular ions. Despite our increasing understanding of the role of ions in cell membrane-related processes the exact molecular details of the mechanisms behind such processes remain elusive. **1.Hector, please deliver the missing citations for this paragraph.**

Direct measurements of ion-membrane interactions in real biological systems are difficult. Simplified lipid bilayers are often used instead as entry-level models to shed light on the role of ions in complex biological membranes [1, 2, 5]. For this reason, interactions of biologically relevant cations, especially Na^+ and Ca^{2+}, with zwitterionic phosphocholine

*samuli.ollila@helsinki.fi

(PC) bilayers have been widely studied in experiments [1–4, 6–9] and classical MD simulations [10–14]. The details of ion binding are, however, not fully consistent in the literature. Non-invasive spectroscopic methods, like nuclear magnetic resonance (NMR), scattering, and infrared spectroscopies mainly suggest that Na^+ ions exhibit negligible binding to PC lipid bilayers. On the contrary, Ca^{2+} is observed to specifically bind to a couple of PC molecules using their phosphate groups [4, 6–9, 15–17]. On the other hand, most atomistic resolution molecular dynamics (MD) simulation models predict a stronger binding for the cations [18]. For example, simulations report Na^+ accumulating in the lipid interface [10] or Ca^{2+} binding up to 4 PC lipids simultaneously, including not only interactions with phosphates but also with carbonyl oxygens [11, 13, 14].

Recent studies within the NMRlipids project (nmrlipids.blogspot.fi) [18] made an attempt to resolve these apparent controversies. A direct comparison of ion binding affinities to PC bilayers between simulations and experiments was performed using the electrometer concept [19]. Namely, the changes in NMR order parameters of the headgroup upon addition of ions is directly compared to the MD simulations results. Analyzing massive amounts of data collected by the Open Collaboration method, it was concluded that the accuracy of the current state of the art lipid models for MD simulations is not sufficient for a detailed interpretation of the interactions of cations with PC lipid bilayers [18].

In this work, we improve the cation binding of a POPC bilayer in MD simulations via the implicit inclusion of the electronic polarizability in the polar region of phospholipids. For this, we apply a simple mean-field electronic continuum correction (ECC) [20] which implies scaling the partial charges of the atoms to account for the missing electronic polarizability in MD simulations. Such an approach has been previously shown to improve the behavior of ions in bulk water simulations [21–24]. As a starting template for our POPC model, we will use the Lipid14 [25]. This force field provides one of the best available descriptions of cation binding [18]. The newly developed ECC-POPC model reproduces the experimentally measurable structural parameters of an ion-free POPC lipid bilayer with the accuracy comparable to the best state of the art lipid models, while improving the membrane binding affinities significantly to sodium and calcium cations.

II. METHODS

A. Electronic continuum correction for lipid bilayers

The lack of electronic polarizability in standard MD simulation force fields has been considered a serious issue since the early days of lipid bilayer simulations. In this work, we circumvent the demanding explicit inclusion of electronic polarization effects [26, 27] by including the electronic part of polarizability in lipid bilayer simulations implicitly via the electronic continuum correction (ECC) [20]. Technically, this is similar to the phenomenological charge-scaling applied in earlier studies of surfactants, lipids or ionic liquids [28–30]. However, the present concept of ECC is physically well justified and rigorously derived [20, 31–33].

According to ECC, the electronic polarizability can be modeled in non-polarizable MD by effectively embedding the ions in a homogeneous dielectric continuum with a dielectric constant ϵ_{el}, which is the electronic part of the dielectric constant of the medium [20]. Following Coulomb's law, ECC can be directly incorporated by scaling the charges with a constant scaling factor of $f_q = \epsilon_{el}^{-1/2}$, giving

$$Q^{ECC} = f_q \cdot Q \qquad (1)$$

for the ECC corrected charges in simulation. Given that the high frequency dielectric constant of water is $\epsilon_{el} = 1.78$ (*i.e.,* the square of the refraction index), the scaling factor for ions in water is roughly $f_q \approx 0.75$. This scaling factor successfully improves the accuracy of simulations of solvated ions, when quantitatively compared with neutron scattering data [21–24]. It is important to note that the high frequency dielectric constant is around 2 for almost any biologically relevant environment [20]. The dielectric discontinuity in a lipid bilayer arises from the orientational polarization of the molecules. Thus, the same correction for the electronic polarizability can be applied throughout the lipid bilayer interface.

While using a scaling factor of $f_q = 0.75$ for ions in water is well justified in the ECC theory [20], it is not clear whether the same factor should be applied to partial charges used to describe molecules in MD models, e.g., lipids in our case. Unlike the total charge of an ion, atomic partial charges within molecules are not physical observables. Several schemes exist for the assignment of partial charges for biomolecules [34], where the restrained electrostatic potential method (RESP) is the most commonly used [35, 36]. Considering that water is often included in RESP calculations or charges are refined to improve certain experimental observables, the electronic polarizability effect of the solvent is included in modern force fields to some extent [35–39]. Thus, the application of the ECC scaling factor, f_q, to the existing partial charges in molecules does not universally follow $f_q = \epsilon_{el}^{-1/2}$. Instead, a consistent scaling factor would lie between the value of 0.75 (*i.e.,* no electronic polarizability included in the original partial charges) and 1 (*i.e.,* electronic polarizability fully included in the original partial charges).

Here we develop ECC-POPC lipid model that accurately describes the binding of sodium and calcium ions to the lipid bilayer. The Lipid14 [25] force field parameters (available in a Gromacs format from Ref. 40) were used as a starting point. This model provides the best response of the head group to ions among the available lipid models (see Figs. 2 and 5 in Ref. 18). Additionally, the Lipid14 model has a relatively realistic head group, glycerol backbone, and acyl chain structure [25, 41]. We applied the ECC correction to the Lipid14 model of POPC by scaling of partial charges of the head group, glycerol backbone, and carbonyl regions. These are the polar parts of phospholipids which can contribute to the cation binding.

To reproduce the experimental ion binding affinities,

we scanned the optimal interval for the scaling factor, $f_q \in (0.75, 1.0)$. The ion binding affinity was evaluated against experiments using the head group order parameters and the electrometer concept [18, 19], as discussed more detail in the next section. In general, scaling down the partial charges reduced the ion binding affinity. We found an optimal binding affinity with the scaling factor of $f_q = 0.8$, which is only slightly higher than the theoretical one ($f_q = 0.75$). Directly applying the 0.8 scaling to the partial charges of the head group, the glycerol backbone, and the carbonyls reduced the area per lipid to 60 Å^2. This area is smaller than in the original Lipid14 model (65.6 ± 0.5 Å^2) [25] and in experiments (64.3 Å^2) [42]. The decrease of the area per lipid arises from a reduced hydration of the lipid head group region after scaling charges which effectively reduces head group polarity. We solve this difficulty by reducing the effective radii of the modified atoms by lowering the σ parameters in the Lennard-Jones potential by a factor of $f_\sigma = 0.89$. The same solution was taken for the ECC-ions in aqueous solvent [21–24]. After reducing the σ parameters, the area per molecule is restored to the experimental value (Table I).

B. Electrometer concept

Comparing MD simulation to NMR experiments, we can validate the ion binding affinity in lipid bilayer simulations using the "electrometer concept" [18, 19]. This method relies on the experimental observation that the C-H bond order parameters of α and β carbons in a PC lipid head group (Fig. 1) are proportional to the amount of charge bound per lipid [19]. The order parameters for all C-H bonds in lipid molecules can be accurately measured using ^{2}H NMR or ^{13}C NMR techniques [43]. From MD simulations the order parameters can be calculated using the definition

$$S_{\mathrm{CH}} = \frac{3}{2}\langle \cos^2\theta - 1 \rangle, \tag{2}$$

where θ is the angle between the C-H bond and membrane normal. Angular brackets point to the average over all sampled configurations.

The relation between the amount of the bound charge per lipid, $X^\pm$, and the head group order parameter change, ΔS^i_{CH}, is empirically quantified as [19, 44]

$$\Delta S^i_{\mathrm{CH}} = S^i_{\mathrm{CH}}(X^\pm) - S^i_{\mathrm{CH}}(0) \approx m_i \frac{4}{3\chi} X^\pm, \tag{3}$$

where i refers to either α or β carbon, $S^i_{\mathrm{CH}}(0)$ denote the order parameter in the absence of bound charge, χ is the quadrupole coupling constant ($\chi \approx 167\,\mathrm{kHz}$), and m_i is a empirical constant depending on the valency and position of the bound charge.

The measured change of the order parameter depends on the head group response to the bound charge and on the amount of the bound charge (*i.e.*, m_i and $X^\pm$ in Eq. 3, respectively). The empirical factor m_i has to be adequately quantified before the electrometer concept can be used to analyze the binding

affinities. This calibration has been done experimentally for a wide range of systems [19, 45]. To calibrate the response of the head group order parameter to the bound charge in simulations, we use experimental data for a strong cationic surfactant dihexadecyldimethylammoniumbromide (DHAB) mixed with a POPC bilayer [46]. DHAB
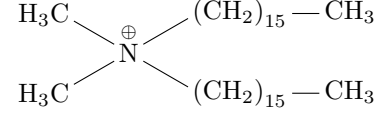
is a cationic surfactant having two acyl chains and bearing a unit charge in the hydrophilic end. Thus, it is expected to locate in the bilayer similarly to the phospholipids, and its molar ratio then gives directly the amount of bound unit charge per lipid $X^\pm$ in these systems [46].

C. Salt concentrations and binding affinity

NMR experiments report the used salt concentrations in two different ways when measuring head group order parameters. Some use the salt concentrations in water before solvating the lipids [6], C_w, while others use atomic absorption spectroscopy and report the salt concentration in the supernatant after the solvation of lipids [7], C_b. In this work, we measure the latter concentration in the aqueous bulk region using the farthest point from the lipid bilayer in the aqueous phase. Notice that former concentration was used by Catte et al. [18]. Although these two definitions vary when applied to Ca^{2+}, they do not significantly affect the conclusions of this work.

To quantify the ion binding affinities to a lipid bilayer, we calculate the relative surface excess of ions with respect to water, Γ^{water}_{ion} [47]. Such a quantity compares the adsorption of ions to the adsorption of water molecules at the interface without the necessity of defining a Gibbs dividing plane between the membrane interior and the water bulk region. In our simulations, we only assume that the interface is located between the ion-free hydrophobic interior of the lipid bilayer and the aqueous region far from the membrane. Such a setup and the above definition of bulk ion concentration provide a simple relation for the relative surface excess Γ^{water}_{ion} for simulations of lipid bilayers,

$$\Gamma^{water}_{ion} = \frac{1}{2A_b}\left(n_{ion} - n_{water}\frac{C_{ion}}{C_{water}}\right). \tag{4}$$

Here, n_{water} and n_{ion} are the total numbers of water molecules and ions in the system, C_{water} and C_{ion} are their respective bulk concentrations in the aqueous phase, and A_b is the area of the unit cell in the membrane plane. The total area of the interface is then twice the area of the membrane, i.e., $2A_b$, because the bilayer has an interface at each of the two leaflets.

D. Validation of lipid bilayer structure against NMR and scattering experiments

The structures of lipid bilayers in simulations without ions were validated against NMR by calculating the order parameters for the C-H bonds and x-ray scattering experiments by the scattering form factors. NMR order parameters validate the structures sampled by the individual lipid molecules with atomic resolution. The simulated order parameters were calculated for all C-H bonds in lipid molecules from Eq. 2. Scattering form factors validate the dimensions of the lipid bilayer (e.g., thickness and area per molecule). Form factors were calculated using

$$F(q) = \int_{-D/2}^{D/2} (\rho_{el}(z) - \rho_{el}^s) \cos(zq_z) \mathrm{d}z, \qquad (5)$$

where $\rho_{el}(z)$ is the total electron density, ρ_{el}^s is the electron density of the solvent far in the aqueous bulk, and z is the distance from the membrane center along its normal with $D/2$ being half of the unit cell size.

E. Simulation details

1. Simulations of POPC bilayers with aqueous ions

Simulations of a POPC bilayer in pure water or at varying salt concentrations consisted of 128 POPC molecules and approximately 50 water molecules per lipid in an orthorhombic simulation box with periodic boundary conditions. The SPC/E [48] water model was used in all ECC-lipid model simulations reported in the main text. This model was also used in the previous parametrization of ECC-ions [21, 22, 24] and its lowered dielectric constant is consistent with the ECC concept [20, 33]. The robustness of our approach with other water models (OPC [49], OPC3 [50], TIP3P [51], TIP3p-FB and TIP4p-FB [52], and TIP4p/2005 [53]) is tested in SI. Sodium, calcium, and chloride ions were modeled as ECC-ions with parameters from Refs. 21, 22. Scaled charges and Lennart-Jones radii for atoms forming the POPC lipid are derived in this work starting from the Lipid14 force field [25]. For comparison, simulations with the Lipid14 model [25] and ion models by Dang and coworkers [54–56] or ECC-ions [21, 22, 24] were also performed. The TIP3p water model [51] was used in all simulations with the original Lipid14 model. **2.Joe, please confirm that this is correct.** Simulation data for the Lipid14 model with Åqvist ions [57] and TIP3P [51] water models were taken directly from Refs. 18, 58–61.

MD simulations were performed using the GROMACS [62] simulation package (version 5.1.4). The simulation parameters used in this work are summarized in Table S1. Combability with openMM simulation package [63] was also tested in SI. The simulated trajectories and parameters files are available at [?] **3.To be uploaded to Zenodo.**

TABLE I: Values of the area per lipid (APL) of POPC bilayers without ions from the Lipid14 simulation ran in this work and from the literature [25], from the ECC-POPC model, and from experiments.

model	APL (Å^2)	Temperature [K]
Lipid14	65.1± 0.6	300
Lipid14 [25]	65.6± 0.5	303
ECC-POPC	63.2± 0.6	300
experiment [42]	64.3	303

2. Simulations of POPC bilayers with cationic surfactants

The topology of dihexadecyldimethylammonium was created with the automated topology builder [64]. The Amber-Tools program [65] was then used to generate the Amber-type force field parameters. These parameters were then converted to the Gromacs format with the acpype tool [66]. The partial charges were then manually modified in the non-scaled version to approximately match similar segments in Lipid14 [25]. For simulation with ECC-POPC, the partial charges of the headgroup were scaled, i.e., $f_q = 0.8$, and the σ of the scale atoms reduced as in POPC-ECC.

The cationic surfactants were randomly mixed among the phospholipids to form bilayer structures with mole fractions of 10%, 20%, 30%, 42%, or 50% of surfactant in the POPC bilayer. All these systems contained 50 POPC molecules per leaflet, 6340 water molecules, and 6, 14, 21, 35, or 50 surfactants per leaflet. Chloride counter ions were used in simulations, while bromide was the counter ion in the experiment [46]. For POPC either the Lipid14 with TIP3P [51] or ECC-POPC with SPC/E [48] were used. The first 20 ns of the total simulation time of 200 ns was considered as an equilibration time and was omitted from the analysis. Sufficient lipid neighbor exchange occurred during the simulations. The trajectories and simulation files for unscaled systems are available from Refs. 67–72.

4.Provide the parameteres for ECC-surfactant somewere.

III. RESULTS AND DISCUSSION

A. Structural parameters of pure ECC-POPC model membrane are in agreement with experiments

First, we present results for bilayers in pure water. The ECC-POPC and Lipid14 models both reproduce the experimental x-ray scattering form factors of a POPC bilayer with a comparable accuracy in Fig. 1. The area per lipid from the Lipid14 model is ≈1Å larger than the experimental value in Table I, while the value from the ECC-POPC model is ≈1Å smaller The values of the area per lipid of the ECC-POPC model show larger variations when simulated with different water models (i.e., 62.2–66.8 Å, see Table S2 in SI), while still being close to the experimentally reported values. We can thus conclude that the ECC-POPC model reproduces the experimental dimensions of the POPC lipid bilayer with the
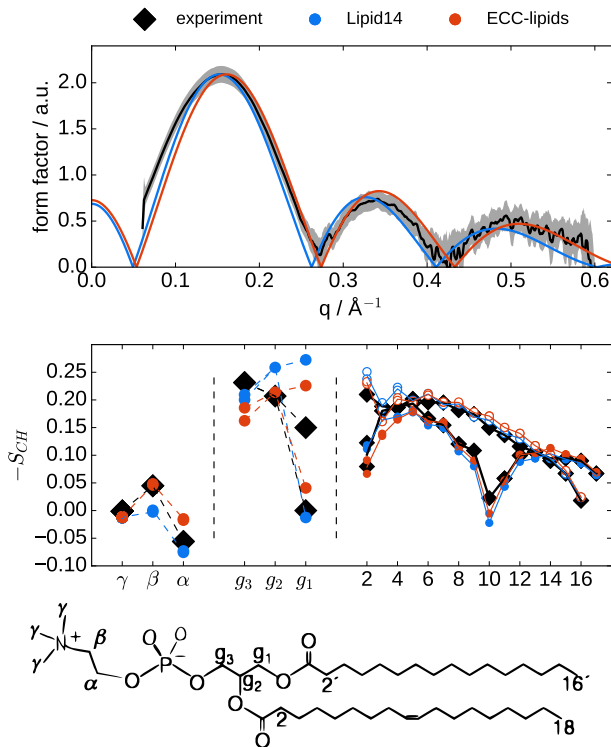
FIG. 1: Top: X-ray scattering form factors from simulations with the Lipid14 [25] and the ECC-POPC models compared with experiments [42] at ??K. Middle: Order parameters of POPC head group, glycerol backbone and acyl chains from simulations with the Lipid14 [25] and the ECC-POPC models compared with experiments [73] at ??K. The size of the markers for the head group order parameters correspond to the error estimate ± 0.02 for experiments [41, 43], while the error estimate for simulations is ± 0.005. The size of the points for acyl chains are decreased by a factor of 3 to improve the clarity of the plot. Bottom: The chemical structure of POPC and the labeling of the carbon segments. Joe, please add the temperatures

comparable accuracy to other state of the art lipid models [43].

Similarly, the acyl chain order parameters of the ECC-POPC model, as well as the Lipid14 model [25], agree with the experimental values within the error bars, as presented in Fig. 1. Notably, the experimentally measured forking and small order parameter values of C_2 segment in sn-2 chain are well reproduced by both models. This feature has been suggested to indicate that the carbonyl of sn-2 chain is directed towards the water phase, in contrast to the carbonyl in sn-1 chain, which would orient more along the bilayer plane [74–76]. While this arrangement may be a relevant feature for the ion binding details, it is not fully reproduced by other available lipid models [43].

The order parameters of the α and β carbons in the headgroup are slightly larger in the ECC-POPC model than in the Lipid14 model, which is apparently related to the P-N vector orienting by about 7° more toward the water phase in the ECC-POPC model, see Fig. 2. Considering the available experimental evidence, it is not possible to suggest which of the two models provides more realistic headgroup orientation.
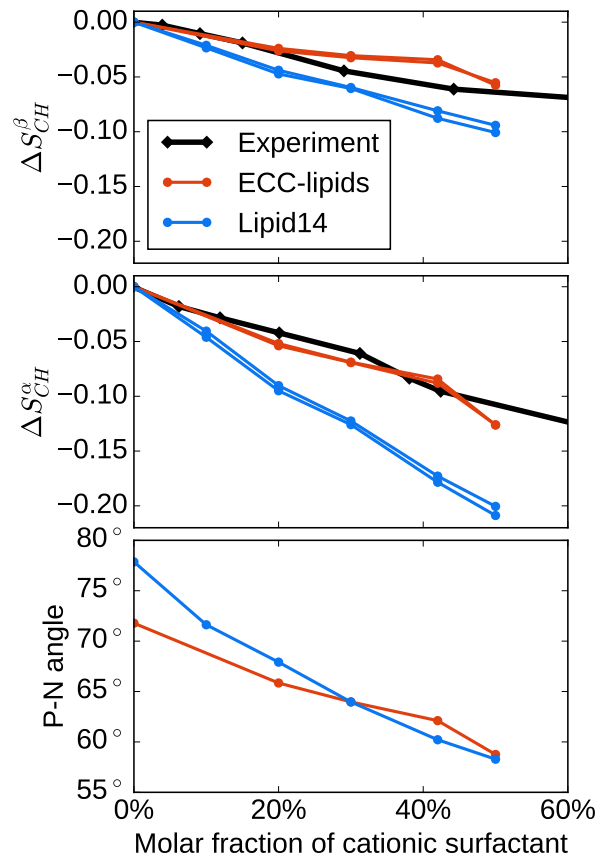

FIG. 2: The changes of headgroup order parameters and P-N vector orientation as a function of a molar fraction of the cationic surfactant dihexadecyldimethylammonium in a POPC bilayer from simulations and experiments [46] at 313 K.

The ECC-POPC model gives the β carbon order parameter value closer to experiments than the Lipid14 model, while the opposite is true for the α carbon. The accuracy of both models in the glycerol backbone region is equally footed with any other state of art lipid model available in literature [41], see Fig. 1.

5.Dynamics check is missing: MSD (Hector/Joe)

B. Calibration of head group response to membrane-bound charge using cationic surfactant

Before studying the sodium and calcium ion binding affinities, we quantify the response of the headgroup order parameters to the amount of bound charge by using mixtures of monovalent cationic surfactants (dihexadecyldimethylammonium) and POPC [46]. These mixtures have a well-defined amount of bound charge per PC, i.e., the molar fraction of cationic surfactants. This direct relation results from the ability of dihexadecyldimethylammonium to be inserted in the lipid bilayers as any lipid because of its two hydrophobic acyl chains. Furthermore, available experimental data for these systems can be used to validate the sensitivity of lipid head-

group order parameters to the amount of bound charge in simulations [46].

The changes of the headgroup order parameters with increasing amount of the cationic surfactant are compared between simulations and experiments [46] in Fig. 2. An approximately linear decrease of the order parameters, as expected from Eq. 3, is observed in both simulations and experiments at least for mole fractions below $\sim 30\%$. The slope is, however, too steep in the Lipid14 model indicating that the response of head group order parameters is too large to the bound positive charge. In contrast, the slope of the ECC-POPC model is in a very good agreement with experiments for the α segment, while being slightly underestimated for the β segment.

In Fig. 2, we show the headgroup P-N vector angle as a function of the mole fraction of the cationic surfactant. As suggested previously [19], the headgroup orients more towards the water phase with the increasing amount of positive charge in a PC lipid bilayer. The effect is more pronounced in the Lipid14 model than in the ECC-POPC model. For example, the addition of 50% mole fraction of the cationic surfactant leads to the decrease of $20°$ of the P-N vector angle for the Lipid14 model while only $11°$ in the ECC-POPC model. The difference is in line with the smaller order parameter changes and the reduced charge–dipole interactions in the latter model. The lower sensitivity of the P-N vector angle response in the ECC-POPC model agrees better with experiments.

C. Validation ECC-POPC model using binding affinities to Na$^+$ and Ca^{2+} Cations: the electrometer concept

Changes of the lipid bilayer head group order parameters from different simulations and experiments [6, 7] are shown in Figs. 3 and 4 as functions of NaCl or CaCl$_2$ concentrations. As seen in Fig. 2, the order parameters decrease proportionally to the amount of the bound positive charge. These results can be thus used to compare the ion binding affinities to lipid bilayers between simulations and experiments using the electrometer concept [18, 19].

The experimentally measured small order parameter changes with NaCl (Fig. 3) are reproduced by the Lipid14 model simulated with Åqvist ions. However, the same combination of models overestimates the order parameter changes with CaCl$_2$ (Fig. 4). Replacing Åqvist ions with ions by Dang et al. [54–56] or ECC-ions [21, 22, 24] did not improve the results (Figs. 3 and 4). In line with the previous work [18], the results suggest that improvements in the lipid parameters are required to correctly describe the binding of cations to phospholipid bilayers.

The results from the simulations combining the ECC-POPC with the ECC-ion models [21, 22, 24] exhibit a significantly improved behavior of the POPC head group order parameters as functions of NaCl or CaCl$_2$ concentrations, see Fig. 3 and Fig. 4. Considering that we can also reproduce the experimental response in systems with known charge density (see above section III B), we conclude that our ECC-model correctly reproduces the binding affinities of Na$^+$ and Ca^{2+} ions to the POPC lipid bilayer. Furthermore, while the response
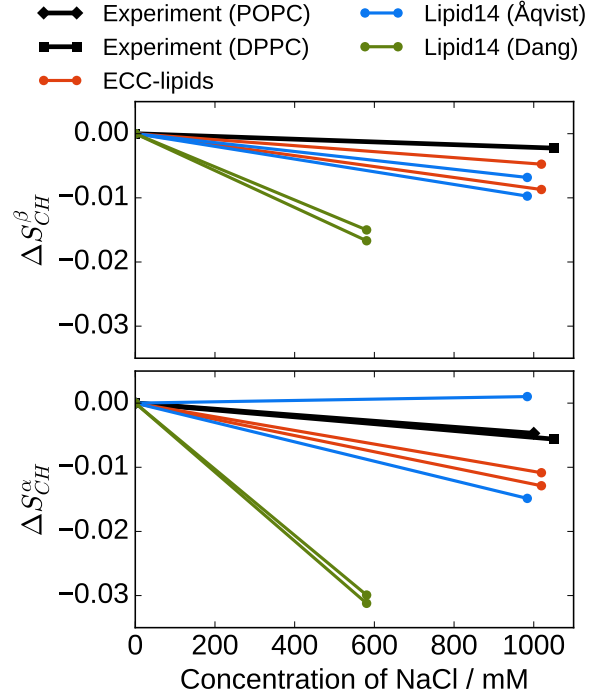

FIG. 3: Changes of the head group order parameters of a POPC bilayer as a function of NaCl concentration in bulk (C_b) from simulations with different force fields at 313 K together with experimental data for DPPC (323 K) [6] and POPC (313 K) [7]. Simulation data with Lipid14 and Åqvist ion parameters at 298 K are taken directly from Refs. [58, 61].

of the glycerol backbone g_3 order parameter to CaCl$_2$ was significantly overestimated in the original Lipid14 model, the ECC-POPC model provides an improved agreement with experiment, as seen in Fig. 4. Also the changes of the P-N vector angle are more pronounced for the Lipid14 model, for which the largest tilting toward water phase induced by a $780\,\mathrm{mM}$ CaCl$_2$ concentration is approximately $17°$. The corresponding value for the ECC-POPC simulation is only $6°$ ($820\,\mathrm{mM}$ CaCl$_2$).

Within the Lipid14 model, the overestimated changes in the lipid headgroup order parameter of POPC as functions of the CaCl$_2$ concentration arise both from the overestimated binding affinity and the excessive sensitivity of the headgroup tilt to the bound positive charge. It is plausible that the same applies to the other lipid models tested in a previous study [18], which underlines the importance to validate the lipid headgroup order parameter response to the bound charge.

Finally, the ion binding affinities for the ECC-POPC model with different water models are compared in SI. In general, the performance of ECC-POPC with any of the water models is better than that of the original Lipid14 model, with the order parameter changes being slightly overestimated with the four-site water models and with TIP3p model.
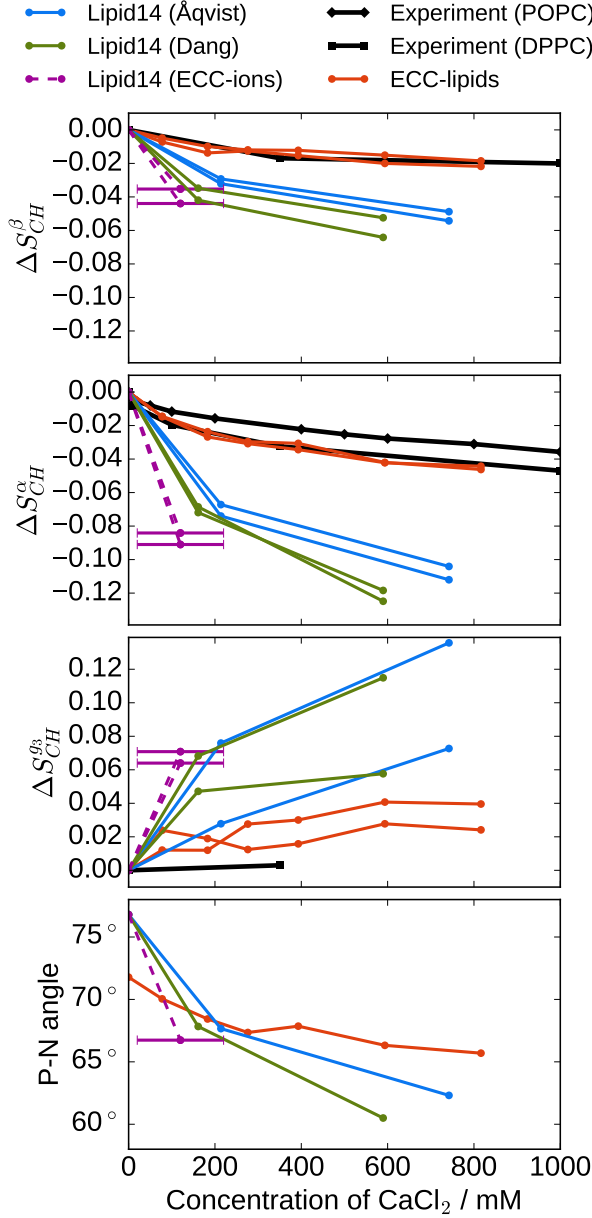
FIG. 4: Changes of the head group order parameters and P-N vector orientation of a POPC bilayer as a function of the CaCl$_2$ concentration in bulk (C_b) from simulations at 313 K together with experimental data (DPPC (323 K) [6] and POPC (313 K) [7]). The error estimate for bulk concentrations was approximately 10 mM. Exception was the order of magnitude larger error in simulation with Lipid14 and ECC-ions due to the unconverged densities (shown if Fig. 5) in too small simulation box. Simulation data with Lipid14 and Åqvist ion parameters at 298 K are taken directly from Refs. [58–60].

D. Binding affinity of Na$^+$ and Ca^{2+} cations to POPC membrane

Binding affinities of Ca^{2+} ions to a POPC bilayer in different simulation models were quantified by calculating the relative surface excess of calcium respect to water molecules,

TABLE II: Bulk concentrations of Ca^{2+} (C_b), relative surface excess of calcium with respect to water (Γ_{Ca}^{water}), and the percetages of Ca^{2+} bound to phosphate or carbonyl oxyges ($r_{PO_4}^{Ca^{2+}}$ and $r_{O_{carb.}}^{Ca^{2+}}$) in different POPC bilayer models. All systems have the same molar concentration of Ca^{2+} respect to water (C_w=350mM). Joe, please confirm that $r_{PO_4}^{Ca^{2+}}$ is really 100% for all the Lipid14 simulations (i.e. that this is not a typo).

model	C_w	C_b / mM	Γ_{Ca}^{water} / nm^{-2}	$r_{PO_4}^{Ca^{2+}}$	$r_{O_{carb.}}^{Ca^{2+}}$
ECC-POPC	350	280 ± 10	0.06 ± 0.01	99%	25%
Lipid14/Åqvist	350	210 ± 10	0.13 ± 0.01	100%	37%
Lipid14/Dang	350	160 ± 10	0.23 ± 0.03	100%	14%
Lipid14/ECC-ions	350	120 ± 100	0.35 ± 0.11	100%	23%

Γ_{ion}^{water}, from Eq. 4. The values of Γ_{ion}^{water} from different POPC simulations with then same molar concetration respect to water (C_w=350mM) are shown in Table II. As expected from the changes of the lipid headgroup order parameters in Fig. 4, the relative surface excess for the ECC-POPC model, Γ_{Ca}^{water} = 0.06 nm^{-2}, is significantly smaller than for the other models, 0.13–0.35 nm^{-2}. Interestingly, the calculated relative surface excess of NaCl at 1 M concentration (ECC-ions [22]) using our POPC-ECC model is not only quantitatively but also qualitatively different from CaCl$_2$ having a negative value $\Gamma_{Na}^{water} = (-0.11 \pm 0.01)$nm^{-2} (Fig. 5). This value means that water molecules are preferred to sodium and chloride ions at the membrane-water interface. This is in contradiction with most of the available lipid force fields, which predict a positive binding of sodium to PC lipid bilayers [18].

E. Molecular interactions between Na$^+$ or Ca^{2+} cations and POPC oxygens

We analyzed the ratio of the number of calcium cations bound to either phosphate or carbonyl moieties and the total number of bound cations in our POPC bilayers as done previously in Ref. 14. A maximum distance of 0.3 nm from any lipid oxygen is used to determine a bound calcium. The results from ECC-POPC simulation in Table II show that almost all (99%) of the bound Ca^{2+} ions are in contact with the phosphate oxygens. From those only one third (32%) also interact with the carbonyl oxygens. The interaction between calcium ions with only carbonyl oxygens is rare (1%). Neither individual lipids nor source chain of carbonyl is distinguished in the analysis. The most likely interactions between Ca^{2+} ions and phosphate oxygens are visualized with the probability density isocontours in Fig. 6. While higher concentrations of CaCl$_2$ increase the number of contacts per lipid, the distribution of contacts between phosphate and carbonyl oxygens is not affected.

Even though Na$^+$ ions do not specifically bind to a POPC bilayer, they still interact mostly with its oxygen moieties. The results from the simulation at 1 M NaCl concentration show that 55% of Na$^+$ ions interact with only phosphate oxygens of POPC and 20% with only carbonyl oxygens, and the rest, 25%, is interacting with both.

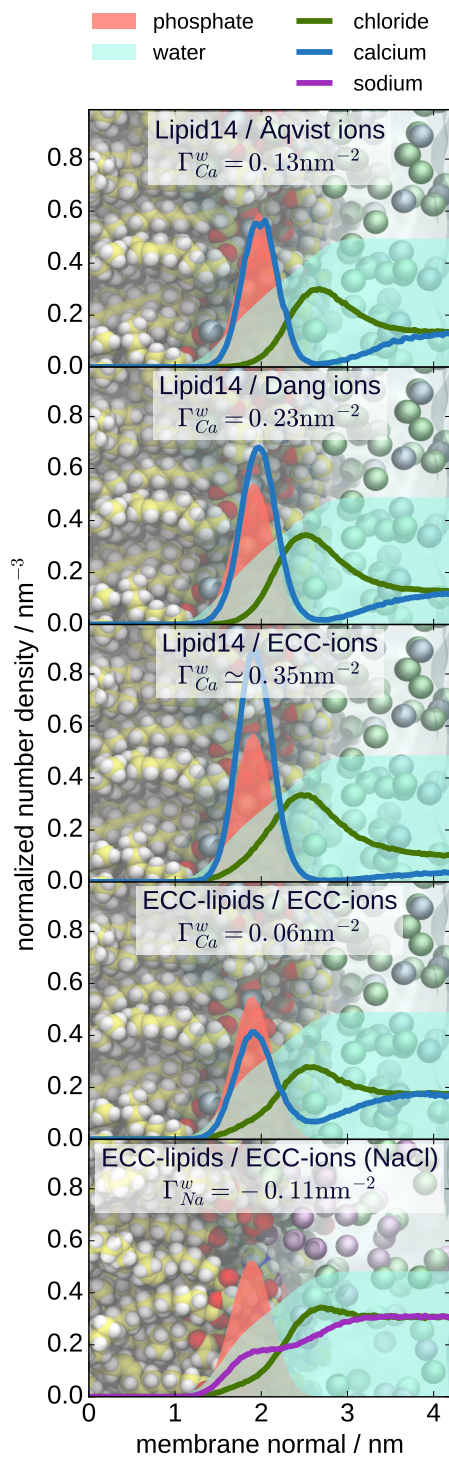FIG. 5: Number density profiles of Ca^{2+}, Na^+ and Cl^- along membrane normal axis for different force fields. Joe, please clarify the sentence below In order to visualize the density profiles with a scale comparable to the profile of Ca^{2+}, densities of Cl^- and Na^+ are divided by 2, and densities of phosphate group resp. water are divided by 5 resp. 200. All the simulations shown here have the same molar concentration of ions in water (C_w=350 mM).
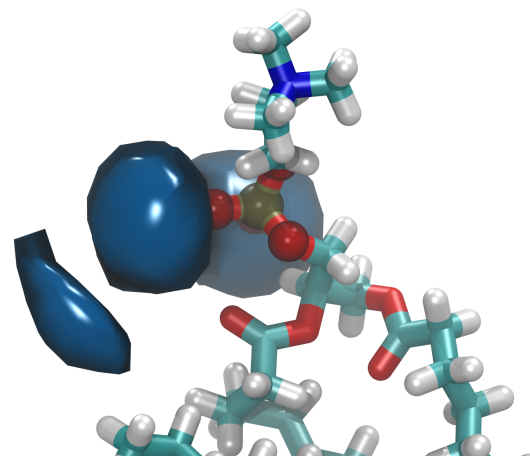

FIG. 6: Isocontours of probability density of Ca^{2+} with respect to the phosphate oxygens of POPC from ECC-POPC simulation. The probability density was evaluated around a single lipid, after its strucutral alignment using only phosphate group.

6.The figure should be updated as discussed last week.

In conclusion, the results suggest that calcium ions bind specifically to phosphate oxygens, occasionally interacting also with carbonyls. This is in good agreement with previous conclusions from several experimental and computational studies [2, 8, 15–17], but suggesting a lower relative binding affinity to the carbonyls than inferred from previous MD simulation studies [10, 11, 13, 14]. Sodium ions also interact primarily with phosphate oxygens of the POPC, but in contrast to calcium, the interactions purely with carbonyls are also significant.

F. Binding stoichiometry of Na$^+$ and Ca^{2+} cations to the POPC membrane

Simple binding models have been used previously to interpret the same experimental data [7, 77] used in this work to validate the simulation models (Fig. 4). In particular, NMR data about PC headgroup order parameters response and atomic absorption spectroscopy were best explained using a ternary complex binding model with a binding stoichiometry of one Ca^{2+} per two POPC lipids [7]. However, a Langmuir adsorption model assuming a Ca^{2+}:POPC stoichiometry of 1:1 also provided a good fit to the experimental data when considering only CaCl$_2$ low concentrations [77].

In this work, we reproduce the same experimental data used to calculate binding stoichiometry with our ECC-POPC model. Using our simulations, we have direct access to exact details of the binding stoichiometry without requiring any middle model as in experiments [7, 77]. To evaluate the relative propensities for each stoichiometric complex (i.e., 1 Ca^{2+}: n POPC), we calculated for each bound Ca^{2+} the number of POPC molecules within a distance of 0.3 nm. Results from the POPC bilayer simulation with a 285 mM bulk concentration of CaCl$_2$ are shown in Fig. 7.
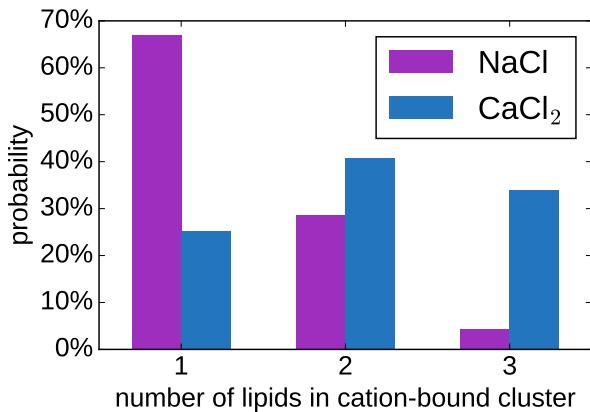
FIG. 7: Relative probabilities of existence of Na$^+$ or Ca^{2+} complexes with a certain number of POPC lipids. Na$^+$ complexes were evaluated from the simulation with 1 M concentration; and Ca^{2+} complexes were evaluated from the simulation with 287 mM concentration.

We found the largest propensity for the 1:2 complex (41%). However, the probabilities of complexes with the stoichiometries of 1:1 (25%) and 1:3 (34%) are only slightly lower. This variability suggests a more complex binding model than the previously considered in a simple ternary complex model. With a broad brushstroke, the simulation data can, however, be viewed such that one calcium binds to two lipids on average, because the probabilities of the complexes with 1 or 3 lipids are almost equal to each other (and complexes with more than three lipids per one calcium ion were not observed). This probably explains why the simple the ternary complex model fits adequately the experimental data, as well as the ECC-POPC simulation results (see Fig. S3 in SI).

The probabilities of different complexes formed by Na$^+$ ions and POPC analyzed from the simulation with the ECC-POPC model at 1 M concentration of NaCl are also shown in Fig. 7. In contrast to calcium, the probability is largest (67%) for 1:1 complex, significantly smaller (29%) for 1:2 complexes and very small (4%) for 1:3 of Na$^+$:POPC complexes.

G. Residence times of Na$^+$ and Ca^{2+} cations in POPC membrane

Equilibration of Ca^{2+} ions at a POPC bilayer in MD simulations is a microsecond time scale process with current state of the art force fields, e.g., CHARMM36 and Slipids force fields [14]. This suggests that at least several microseconds are required to reach the binding/unbinding equilibrium. To quantify the exchange of ions between the membrane and solvent in simulations, we thus calculated residence times of ions bound to the membrane. In our analysis, an ion is considered to be bound when it is within 0.3 nm from any oxygen atom belonging to a POPC molecule. **7.HECTOR: I do fully understand the content of this paragraph. I will discuss this with Joe tomorrow. Please be carefull with my changes.** The his-

tograms of residence times of Ca^{2+} (C_w = 450 mM) in a POPC bilayer for simulations using either ECC-POPC or CHARMM36 (Simulation from Refs. 14, 78) are shown in Fig. S4 in SI. In the CHARMM36 simulation, a significant number of the calciums are bound for the whole length of the trajectory (800 ns). In contrast, at least an order of magnitude faster bound/unbound calcium exchange is observed within the ECC-POPC model, where 90% of the Ca^{2+} residence times to a POPC membrane are shorter than 60 ns. The longest observed residence time is around 150 ns, which is well below the total length of the simulation used for analysis, i.e., 200 ns. Note that these results are in line with the experimental estimate that the residence time of Ca^{2+} at each PC headgroup is shorter than 10 μs [7]. The exchange of Na$^+$ ions at the POPC membrane is another order of magnitude faster, yielding 90% of the residence times smaller than 1 ns, with the longest residence time being 6 ns.

In conclusion, the results from the ECC-POPC model suggest that the exchange of calcium between the POPC bilayer and the solvent occurs within $\sim$100 ns timeframe, which is significantly faster than observed in most of the available lipid models [14]. Sodium cations exhibit an even a more rapid exchange. This all suggests that simulations with a length of several hundreds of nanoseconds are sufficient to simulate ion binding to phospholipid bilayers in equilibrium when realistic force fields are used. This has not been the case with previous lipid force fields, which overestimate the binding strength of the sodium and calcium cations [14, 18].

IV. CONCLUSIONS

In this study, we employed the electrometer concept to demonstrate that the binding of Na$^+$ and Ca^{2+} ions to a POPC lipid bilayer can be accurately described within a classical MD simulation force field, provided that electronic polarization is implicitly included via the electronic continuum correction [20]. While the structural details of a POPC lipid bilayer simulated with the newly developed ECC-POPC model agree with experiments with an accuracy comparable to the other state of the art lipid models, the model also reproduces the experimental lipid head group order parameter responses to a cationic surfactant, NaCl, and CaCl$_2$ concentrations. It thus represents a significant improvement over other available lipid models, which overestimate cation binding affinities [18]. The ECC-POPC model is built upon the Lipid14 POPC model [25] by scaling the partial charges by a factor of 0.8 and reducing the Lennart-Jones radii by a factor of 0.89 for the headgroup, glycerol backbone, and carbonyl atoms.

The good agreement with experiments enables us to interpret NMR experiments with atomistic details using MD simulations with the ECC-lipid model. In line with previous interpretations of experimental data [8, 15–17], Ca^{2+} ions interact mainly with phosphate oxygens. However, the stoichiometry of calcium binding is significantly more complicated than the simple ternary complex model, used to interpret NMR data, where one calcium binds to two POPC molecules [7]. While complexes with one calcium ion bound to two lipids are the

most probable also in the ECC-POPC model, complexes of one or three lipids per one calcium were observed to relatively abundant and also almost equally likely. While the success of the simple ternary complex model in fitting NMR data is understandable based on the simulation results, it cannot capture the complex nature of calcium binding to phospholipid bilayers observed in the present simulation.

Accurate description of cation binding to POPC bilayer paves the way for simulations of complex biochemical systems at cellular membranes with realistically described electrostatic interactions. To this end, the compatibility of the ECC-POPC model with existing models for proteins and other biological molecules should be verified and, if necessary, further adjustments following ECC concept to the force fields of the interacting molecules with the lipids should be addressed.

This work can be reached as a repository containing all data at `zenodo.org:\dots\dots\dots`.

[1] J. Seelig, Cell Biol. Int. Rep. **14**, 353 (1990), URL http://dx.doi.org/10.1016/0309-1651(90)91204-H.

[2] G. Cevc, Biochim. Biophys. Acta - Rev. Biomemb. **1031**, 311 (1990).

[3] J.-F. Tocanne and J. Teissié, Biochim. Biophys. Acta - Reviews on Biomembranes **1031**, 111 (1990).

[4] G. Pabst, A. Hodzic, J. Strancar, S. Danner, M. Rappolt, and P. Laggner, Biophys. J. **93**, 2688 (2007).

[5] P. Scherer and J. Seelig, The EMBO journal **6** (1987).

[6] H. Akutsu and J. Seelig, Biochemistry **20**, 7366 (1981).

[7] C. Altenbach and J. Seelig, Biochemistry **23**, 3913 (1984).

[8] H. Binder and O. Zschörnig, Chem. Phys. Lipids **115**, 39 (2002).

[9] D. Uhrkov, N. Kuerka, J. Teixeira, V. Gordeliy, and P. Balgav, Chemistry and Physics of Lipids **155**, 80 (2008).

[10] R. A. Böckmann, A. Hac, T. Heimburg, and H. Grubmüller, Biophys. J. **85**, 1647 (2003).

[11] R. A. Böckmann and H. Grubmüller, Ang. Chem. Int. Ed. **43**, 1021 (2004).

[12] M. L. Berkowitz and R. Vacha, Acc. Chem. Res. **45**, 74 (2012).

[13] A. Melcrov, S. Pokorna, S. Pullanchery, M. Kohagen, P. Jurkiewicz, M. Hof, P. Jungwirth, P. S. Cremer, and L. Cwiklik, Sci. Reports **6**, 38035 (2016).

[14] M. Javanainen, A. Melcrova, A. Magarkar, P. Jurkiewicz, M. Hof, P. Jungwirth, and H. Martinez-Seara, Chem. Commun. **53**, 5380 (2017), URL http://dx.doi.org/10.1039/C7CC02208E.

[15] H. Hauser, M. C. Phillips, B. Levine, and R. Williams, Nature **261**, 390 (1976).

[16] H. Hauser, W. Guyer, B. Levine, P. Skrabal, and R. Williams, Biochim. Biophys. Acta - Biomembranes **508**, 450 (1978), ISSN 0005-2736, URL http://www.sciencedirect.com/science/article/pii/0005273678900913.

[17] L. Herbette, C. Napolitano, and R. McDaniel, Biophys. J. **46**, 677 (1984).

[18] A. Catte, M. Girych, M. Javanainen, C. Loison, J. Melcr, M. S. Miettinen, L. Monticelli, J. Maatta, V. S. Oganesyan, O. H. S. Ollila, et al., Phys. Chem. Chem. Phys. **18** (2016).

[19] J. Seelig, P. M. MacDonald, and P. G. Scherer, Biochemistry **26**, 7535 (1987).

[20] I. Leontyev and A. Stuchebrukhov, Phys. Chem. Chem. Phys. **13**, 2613 (2011).

[21] T. Martinek, E. Duboué-Dijon, S. Timr, P. E. Mason, K. Baxová, H. E. Fischer, B. Schmidt, E. Pluhařová, and P. Jungwirth, *Calcium ions in aqueous solutions: Accurate force field description aided by ab initio molecular dynamics and neutron scattering* (2017), submitted.

[22] E. Pluhaová, H. E. Fischer, P. E. Mason, and P. Jungwirth, Molecular Physics **112**, 1230 (2014), ISSN 0026-8976, URL http://www.tandfonline.com/doi/abs/10.1080/00268976.2013.875231.

[23] M. Kohagen, P. E. Mason, and P. Jungwirth, J. Phys. Chem. B **118**, 7902 (2014).

[24] M. Kohagen, P. E. Mason, and P. Jungwirth, J. Phys. Chem. B **120**, 1454 (2016).

[25] C. J. Dickson, B. D. Madej, . A. Skjevik, R. M. Betz, K. Teigen, I. R. Gould, and R. C. Walker, J. Chem. Theory Comput. **10**, 865 (2014).

[26] T. R. Lucas, B. A. Bauer, and S. Patel, Biochimica et Biophysica Acta (BBA) - Biomembranes **1818**, 318 (2012), membrane protein structure and function.

[27] J. Chowdhary, E. Harder, P. E. M. Lopes, L. Huang, A. D. MacKerell, and B. Roux, J. Phys. Chem. B **117**, 9142 (2013).

[28] B. Jonsson, O. Edholm, and O. Teleman, J. Chem. Phys. **85**, 2259 (1986).

[29] E. Egberts, S.-J. Marrink, and H. J. C. Berendsen, European Biophysics Journal **22**, 423 (1994).

[30] W. Beichel, N. Trapp, C. Hauf, O. Kohler, G. Eickerling, W. Scherer, and I. Krossing, Angewandte Chemie International Edition **53**, 3143 (2014), ISSN 1521-3773, URL http://dx.doi.org/10.1002/anie.201308760.

[31] I. V. Leontyev and A. A. Stuchebrukhov, The Journal of chemical physics **130**, 085102 (2009), ISSN 1089-7690, URL http://scitation.aip.org/content/aip/journal/jcp/130/8/10.1063/1.3060164.

[32] I. V. Leontyev and A. A. Stuchebrukhov, Journal of Chemical Theory and Computation **6**, 1498 (2010), ISSN 1549-9618, URL http://dx.doi.org/10.1021/ct9005807.

[33] I. V. Leontyev and A. A. Stuchebrukhov, Journal of Chemical Physics **141**, 014103 (2014), ISSN 00219606, 1504.07652, URL http://aip.scitation.org/doi/10.1063/1.4884276.

[34] H. Hu, Z. Lu, and and Weitao Yang*, Journal of Chemical Theory and Computation **3**, 1004 (2007), ISSN 1549-9618, URL

http://dx.doi.org/10.1021/ct600295n.

[35] C. C. I. Bayly, P. Cieplak, W. D. Cornell, and P. a. Kollman, The Journal of Physical ... **97**, 10269 (1993), ISSN 0022-3654, 93/2091- 10269$04.00/0, URL http://pubs.acs.org/doi/abs/10.1021/j100142a004.

[36] U. C. Singh and P. A. Kollman, Journal of Computational Chemistry **5**, 129 (1984), ISSN 1096987X.

[37] W. L. Jorgensen, D. S. Maxwell, and J. Tirado-Rives, J. Am. Chem. Soc. **118**, 11225 (1996).

[38] D. S. Cerutti, J. E. Rice, W. C. Swope, and D. A. Case, The Journal of Physical Chemistry B **117**, 2328 (2013), pMID: 23379664, http://dx.doi.org/10.1021/jp311851r, URL http://dx.doi.org/10.1021/jp311851r.

[39] A. L. Benavides, M. A. Portillo, V. C. Chamorro, J. R. Espinosa, J. L. F. Abascal, and C. Vega, The Journal of Chemical Physics **147**, 104501 (2017).

[40] O. H. S. Ollila and M. Retegan, *Md simulation trajectory and related files for popc bilayer (lipid14, gromacs 4.5)* (2014), URL http://dx.doi.org/10.5281/zenodo.12767.

[41] A. Botan, F. Favela-Rosales, P. F. J. Fuchs, M. Javanainen, M. Kanduč, W. Kulig, A. Lamberg, C. Loison, A. Lyubartsev, M. S. Miettinen, et al., J. Phys. Chem. B **119**, 15075 (2015).

[42] N. Kučerka, M. P. Nieh, and J. Katsaras, Biochim. Biophys. Acta **1808**, 2761 (2011), ISSN 0006-3002.

[43] O. S. Ollila and G. Pabst, *Atomistic resolution structure and dynamics of lipid bilayers in simulations and experiments* (2016), in Press, URL http://dx.doi.org/10.1016/j.bbamem.2016.01.019.

[44] T. M. Ferreira, R. Sood, R. Bärenwald, G. Carlström, D. Topgaard, K. Saalwächter, P. K. J. Kinnunen, and O. H. S. Ollila, Langmuir **32**, 6524 (2016).

[45] G. Beschiaschvili and J. Seelig, Biochim. Biophys. Acta - Biomembranes **1061**, 78 (1991).

[46] P. G. Scherer and J. Seelig, Biochemistry **28**, 7720 (1989).

[47] D. K. Chattoraj and K. S. Birdi, *Adsorption at the Liquid Interface from the Multicomponent Solution* (Springer US, Boston, MA, 1984), pp. 83–131, ISBN 978-1-4615-8333-2, URL https://doi.org/10.1007/978-1-4615-8333-2_4.

[48] H. J. C. Berendsen, J. R. Grigera, and T. P. Straatsma, Journal of Physical Chemistry **91**, 6269 (1987), ISSN 0022-3654, URL http://links.isiglobalnet2.com/gateway/Gateway.cgi?GWVersion=2{\&}SrcAuth=mekentosj{\&}SrcApp=Papers{\&}DestLinkType=FullRecord{\&}DestApp=WOS{\&}KeyUT=A1987K994100038{\%}5Cnpapers2://publication/uuid/17978EF7-93C9-4CB5-89B3-086E5D2B9169{\%}5Cnhttp://pubs.acs.org/doi/pdf/10.1021/.

[49] S. Izadi, R. Anandakrishnan, and A. V. Onufriev, The Journal of Physical Chemistry Letters **5**, 3863 (2014), ISSN 1948-7185, 1408.1679, URL http://pubs.acs.org/doi/10.1021/jz501780a.

[50] S. Izadi and A. V. Onufriev, Journal of Chemical Physics **145**, 074501 (2016), ISSN 00219606, URL http://aip.scitation.org/doi/10.1063/1.4960175.

[51] W. L. Jorgensen, J. Chandrasekhar, J. D. Madura, R. W. Impey, and M. L. Klein, J. Chem. Phys **79**, 926 (1983).

[52] L. P. Wang, T. J. Martinez, and V. S. Pande, Journal of Physical Chemistry Letters **5**, 1885 (2014), ISSN 19487185, URL http://pubs.acs.org/doi/abs/10.1021/jz500737m.

[53] J. L. Abascal and C. Vega, The Journal of chemical physics **123**, 234505 (2005), ISSN 00219606, URL http://aip.scitation.org/doi/10.1063/1.2121687.

[54] D. E. Smith and L. X. Dang, J. Chem. Phys **100**, 3757 (1994), URL http://scitation.aip.org/content/aip/journal/jcp/100/5/10.1063/1.466363.

[55] T.-M. Chang and L. X. Dang, J. Phys. Chem. B **103**, 4714 (1999), ISSN 1520-6106, URL http://dx.doi.org/10.1021/jp982079o.

[56] L. X. Dang, G. K. Schenter, V.-A. Glezakou, and J. L. Fulton, J. Phys. Chem. B **110**, 23644 (2006), ISSN 1520-6106, URL http://dx.doi.org/10.1021/jp064661f.

[57] J. Aaqvist, J. Phys. Chem. **94**, 8021 (1990), http://dx.doi.org/10.1021/j100384a009, URL http://dx.doi.org/10.1021/j100384a009.

[58] M. Girych and O. H. S. Ollila, *Popc_amber_lipid14_verlet* (2015), URL http://dx.doi.org/10.5281/zenodo.30898.

[59] M. Girych and O. H. S. Ollila, *Popc_amber_lipid14_cacl2_035mol* (2015), URL http://dx.doi.org/10.5281/zenodo.34415.

[60] M. Girych and S. Ollila, *Popc_amber_lipid14_cacl2_035mol* (2016), URL https://doi.org/10.5281/zenodo.46234.

[61] M. Girych and O. H. S. Ollila, *Popc_amber_lipid14_nacl_1mol* (2015), URL http://dx.doi.org/10.5281/zenodo.30865.

[62] M. J. Abraham, T. Murtola, R. Schulz, S. Páll, J. C. Smith, B. Hess, and E. Lindah, SoftwareX **1-2**, 19 (2015), ISSN 23527110, URL http://www.sciencedirect.com/science/article/pii/S2352711015000059.

[63] P. Eastman, J. Swails, J. D. Chodera, R. T. McGibbon, Y. Zhao, K. A. Beauchamp, L.-P. Wang, A. C. Simmonett, M. P. Harrigan, C. D. Stern, et al., PLOS Computational Biology **13**, e1005659 (2017), ISSN 1553-7358, URL http://dx.plos.org/10.1371/journal.pcbi.1005659.

[64] A. K. Malde, L. Zuo, M. Breeze, M. Stroet, D. Poger, P. C. Nair, C. Oostenbrink, and A. E. Mark, Journal of Chemical Theory and Computation **7**, 4026 (2011).

[65] D. Case, D. Cerutti, T. Cheatham, III, T. Darden, R. Duke, T. Giese, H. Gohlke, A. Goetz, D. Greene, et al., *AMBER 2017* (2017), university of California, San Francisco.

[66] A. W. SOUSA DA SILVA and W. F. VRANKEN, *ACPYPE - AnteChamber PYthon Parser interfacE.* (2017), manuscript submitted.

[67] O. H. S. Ollila, *POPC bilayer simulated at T313K with the Lipid14 model using Gromacs* (2017), URL https://doi.org/10.5281/zenodo.1020709.

[68] O. H. S. Ollila, *POPC bilayer with 10% of dihexadecyldimethylammonium simulated at T313K with the Lipid14 model using Gromacs* (2017), URL https://doi.org/10.5281/zenodo.1020240.

[69] O. H. S. Ollila, *POPC bilayer with 20% of dihexadecyldimethylammonium simulated at T313K with the Lipid14 model using Gromacs* (2017), URL https://doi.org/10.5281/zenodo.1020593.

[70] O. H. S. Ollila, *POPC bilayer with 30% of dihexadecyldimethylammonium simulated at T313K with the Lipid14 model using Gromacs* (2017), URL https://doi.org/10.5281/zenodo.1020623.

[71] O. H. S. Ollila, *POPC bilayer with 42% of dihexadecyldimethylammonium simulated at T313K with the Lipid14 model using Gromacs* (2017), URL https://doi.org/10.5281/zenodo.1020671.

[72] O. H. S. Ollila, *POPC bilayer with 50% of dihexadecyldimethy-*

lammonium simulated at T313K with the Lipid14 model using Gromacs (2017), URL `https://doi.org/10.5281/zenodo.1020689`.

[73] T. M. Ferreira, F. Coreta-Gomes, O. H. S. Ollila, M. J. Moreno, W. L. C. Vaz, and D. Topgaard, Phys. Chem. Chem. Phys. **15**, 1976 (2013).

[74] A. Seelig and J. Seelig, Biochim. Biophys. Acta **406**, 1 (1975).

[75] H. Schindler and J. Seelig, Biochemistry **14**, 2283 (1975).

[76] K. Gawrisch, D. Ruston, J. Zimmerberg, V. Parsegian, R. Rand, and N. Fuller, Biophys. J. **61**, 1213 (1992).

[77] P. M. Macdonald and J. Seelig, Biochemistry **26**, 1231 (1987).

[78] M. Javanainen, *POPC with varying amounts of cholesterol, 450 mM of CaCl_2. Charmm36 with ECC-scaled ions* (2017), URL `https://doi.org/10.5281/zenodo.259376`.

ToDo

P.

1. Hector, please deliver the missing citations for this paragraph. 1
2. Joe, please confirm that this is correct. 4
3. To be uploaded to Zenodo 4
4. Provide the parameteres for ECC-surfactant somewere. 4
5. Dynamics check is missing: MSD (Hector/Joe) . . . 5
6. The figure should be updated as discussed last week. 8
7. HECTOR: I do fully understand the content of this paragraph. I will discuss this with Joe tomorrow. Please be carefull with my changes. 9